SCIENTIFIC REPORTS

OPEN

SUBJECT AREAS:
NANOBIOTECHNOLOGY
CHEMICAL MODIFICATION
NANOSTRUCTURES
POLYMERS

Received
1 March 2013

Accepted
24 April 2013

Published
15 May 2013

Correspondence and requests for materials should be addressed to C.B.M. (cbmao@ou.edu)

Virus-based Photo-Responsive Nanowires Formed By Linking Site-Directed Mutagenesis and Chemical Reaction

Murali Murugesan, Gopal Abbineni, Susan L. Nimmo, Binrui Cao & Chuanbin Mao

Department of Chemistry & Biochemistry, Stephenson Life Sciences Research Center, University of Oklahoma, 101 Stephenson Parkway, Norman, Oklahoma 73019, USA.

Owing to the genetic flexibility and error-free bulk production, bio-nanostructures such as filamentous phage showed great potential in materials synthesis, however, their photo-responsive behaviour is neither explored nor unveiled. Here we show M13 phage genetically engineered with tyrosine residues precisely fused to the major coat protein is converted into a photo-responsive organic nanowire by a site-specific chemical reaction with an aromatic amine to form an azo dye structure on the surface. The resulting azo-M13-phage nanowire exhibits reversible photo-responsive properties due to the photo-switchable cis-trans isomerisation of the azo unit formed on the phage. This result shows that site-specific display of a peptide on bio-nanostructures through site-directed genetic mutagenesis can be translated into site-directed chemical reaction for developing advanced materials. The photo-responsive properties of the azo-M13-phage nanowires may open the door for the development of light controllable smart devices for use in non-linear optics, holography data storage, molecular antenna, and actuators.

M13 bacteriophage (also called phage), a naturally occurring nanowire-like virus (~900 nm long and 7 nm wide, Fig. 1a) that specifically infects bacteria, is a non-toxic, genetically modifiable monodisperse biopolymer, which can be easily replicated and amplified in bulk in gram negative bacteria[1–12]. Traditional phage display, display of a foreign peptide on a phage particle using molecular cloning, can be used to selectively display short amino acid sequences on the surface of major coat (side wall) or minor coat (tip) of virus without compromising its infectivity[13–15]. However, such genetically engineered virus has not been applied to achieve site-direct chemical modification to impart smart functionalities to virus. Although it is possible to chemically modify wild-type phage[10], the introduction of foreign peptides to the solvent-exposed domain of the coat protein by phage display technique will increase the accessibility and allow the exposure of functional groups to the solution for chemical reaction with other organic molecules.

Photo-responsive materials are those that can respond to different wavelengths of the light or undergo changes in structures or properties upon exposure to a particular wavelength of light. Azo compounds are molecules bearing the functional group R-N=N-R′, where R and R′ are either aryl or alkyl and the N=N double bond is called an azo group[16–18]. They include two isomers, cis and trans, due to the restricted rotation of the chemical bonds around the N=N double bond. In the cis isomer, both R and R′ groups are locked on the same side of the N=N double bond, whereas in the trans isomer, both R and R′ groups are locked on the opposite sides of the N=N double bond (Fig. 2a). Azo compounds have been applied to develop photo-responsive polymers using different approaches, such as doping polymers with azo as well as non-covalent or covalent attachment of azo onto the main chain, side chain or dendritic polymer framework[17]. The reversible photo-induced cis-trans isomerisation of the azo chromophore upon light exposure in the azo polymers can cause significant bulk and surface property changes. This photo-responsive behaviour is the foundation of using the azo polymers in reversible data storage, non-linear optics and holography data storage[16–18].

Earlier researchers attempted to conjugate organic and biological molecules to develop novel photo-responsive materials. Some researchers have used biomolecules such as proteins to make photo-responsive agents by conjugation with azo polymer[16]. For example, upon conjugating the azo polymer onto an enzyme, the enzyme underwent a reversible change in size and hydrophobicity upon exposure to light. The resulting photo-responsive

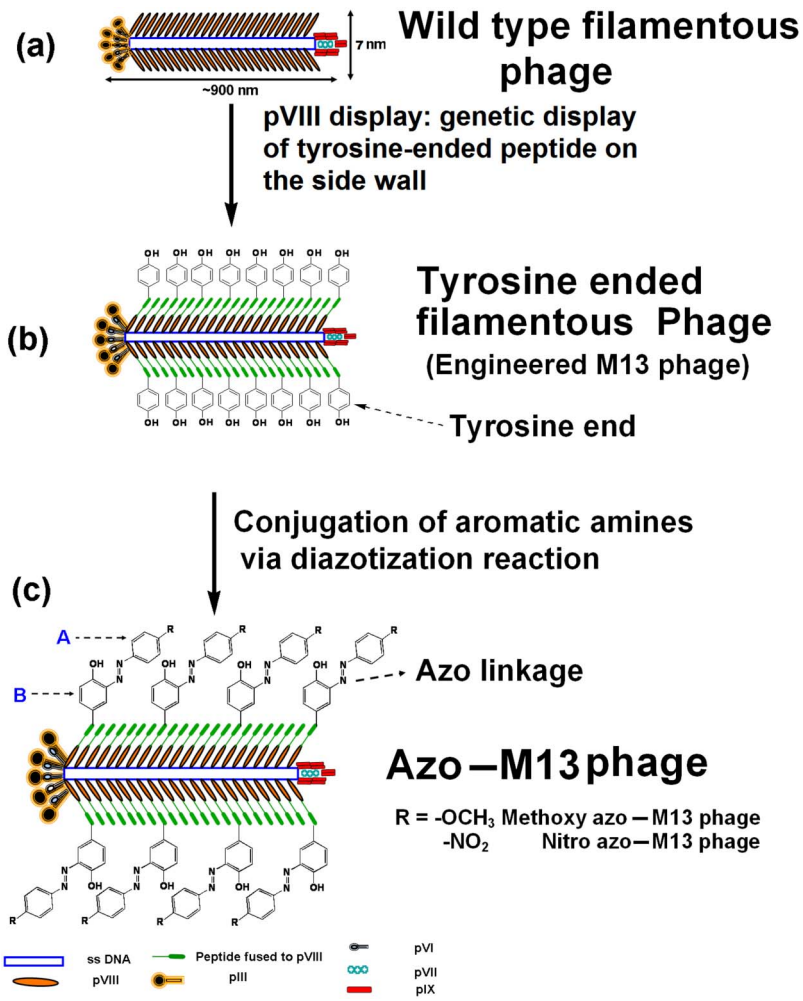

Figure 1 | The general idea of this work. Conversion of wild type M13 phage (a) into tyrosine-ended M13 phage (Engineered M13 phage) (b) via site-directed genetic mutagenesis through phage display technique. In phage display technique, a tyrosine-terminated decapeptide with a sequence of Y-Y-G-Y-Y-G-Y-Y-G-Y is genetically fused to the N terminus of major coat protein (pVIII) of wild type phage. The aromatic amines will be conjugated with the tyrosine ring on the tyrosine-terminated phage through the well-known diazotization reaction. This bioconjugation approach thus offers an easy way to develop photo-responsive azo-M13 phage nanowires (c). Ring A and B are from the aromatic amine and tyrosine, respectively, and are indicated in the Figure. They are confirmed by FTIR (Fig. S4) and NMR (Figs. 5 and S5) spectra.

agent served as a molecular antennae and actuator to reversibly turn the enzyme activity *on* and *off* in response to distinct wavelengths of light with sharp control in reversibility[18]. Similarly, the photo-responsive behaviour of cyclic octapeptides conjugated with azo end groups[19] and azobenzene-functionalized dendritic lysine peptides were also studied[20]. Furthermore, a proline-based azobenzene peptide for holographic optical data storage was also reported[21]. However, the biomolecules studied so far were limited to either enzymes or peptides that lack well-defined secondary or tertiary architecture and thus cannot result in higher-order structures for device applications. Moreover, in most approaches to the synthesis of the azo-based polymers or biomolecules, the azo unit is pre-synthesized and conjugated into the polymers or biomolecules. Here, we show the natural formation of azo group by direct conjugation of aromatic amine group to tyrosine genetically displayed on the side wall (major coat) of filamentous phage (Fig. 1).

Results

Architecture of filamentous virus and synthesis of Azo-M13 phage nanowires. Due to its shape anisotropy and monodispersity, M13 phage can serve as a building block in supramolecular assembly to form 2D and 3D ordered materials through a lyotropic liquid crystalline behaviour. The typical structure of M13 virus is made of ~2,700 highly ordered copies of the major coat protein (called pVIII, constituting the side wall of phage) surrounding a circular single-stranded DNA genome (Fig. 1a)[22]. It has a molecular mass about ~500 kDa, of which 88% is protein and 12% is DNA. There are five copies each of minor coat proteins, pIII and pVI at one end of the viral particle whereas there are five copies each of other two minor coat proteins, pVII and pIX at the other end. Thus, in essence the virus can be envisioned as a monodisperse biopolymer. All the coat proteins on the virus are encoded by DNA inside the phage. Thus, by inserting a foreign peptide into the gene of virus, a unique sequence can be site-specifically displayed on the virus coat. Hence, by displaying a unique sequence on the viral particle, the available chemical groups for conjugation greatly vary. As a result, custom designed genetically engineered virus can provide unique interaction sites to further enable the site-directed conjugation of other organic functional groups to the phage.

So far, there is no report on the conjugation of phage with photo-responsive functional organic groups. Here, we observed the formation of azo by interacting an aromatic amine with a peptide Y-Y-G-Y-Y-G-Y-Y-G-Y displayed on the side wall of M13 phage (Fig. 1 a–c). It should be noted that Y-Y-G-Y-Y-G-Y-Y-G-Y sequence is displayed on the major coat of M13 phage by genetic means (Fig. S1), creating an ideal environment for electrophilic and

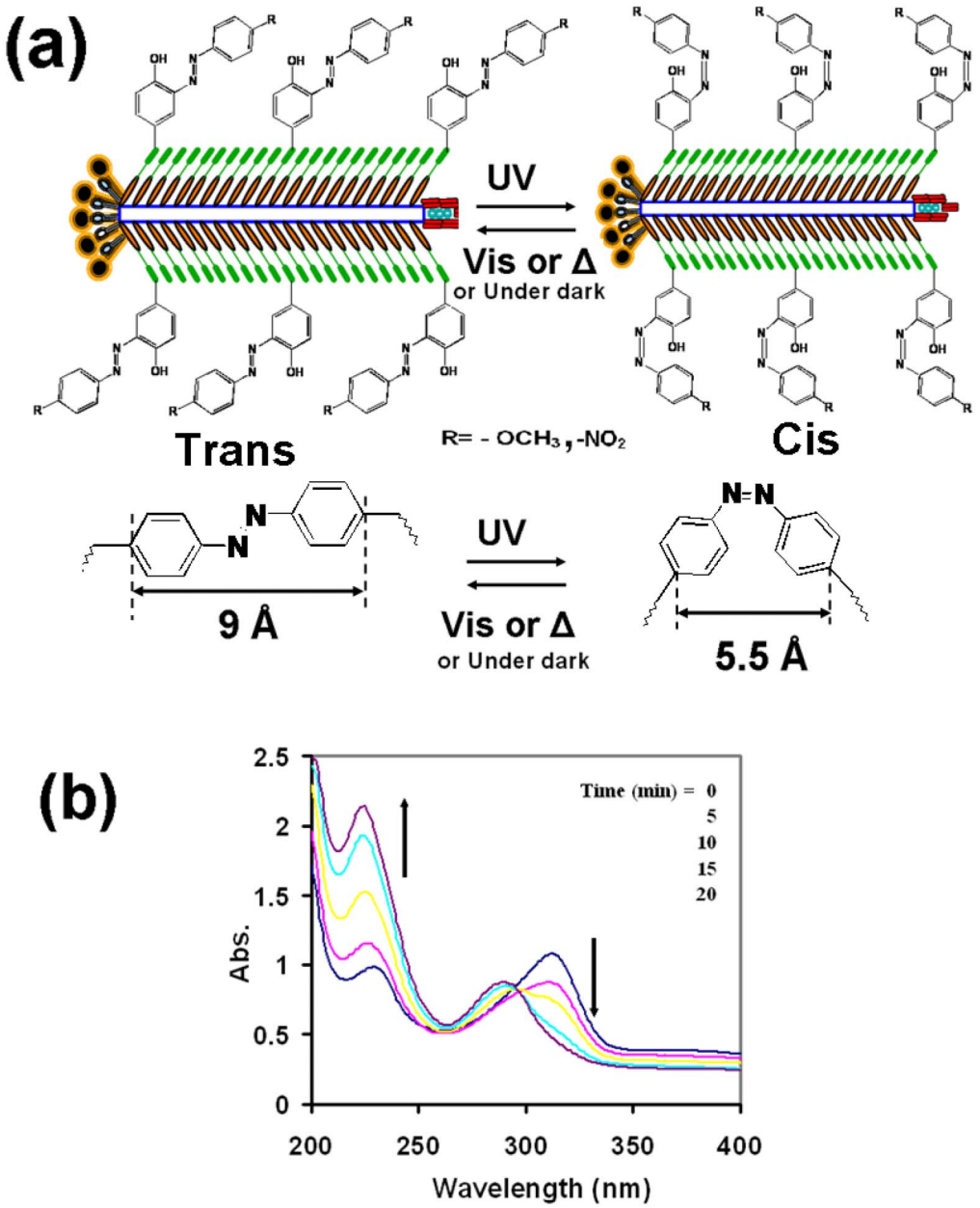

Figure 2 | Schematic representation (a) of novel photo-responsive azo-M13 phage and reversible photo-isomerization under UV exposure (b) and dark condition (Fig. 3) (R = $-OCH_3$ or $-NO_2$). (a) The cartoon is not to scale because phage is a giant architecture (~900 nm long and 7 nm wide) in comparison to the azo units. For the sake of clarity only a few tyrosine molecules are shown on the phage. (b) Change in the absorption spectra (200–400 nm) of the methoxy-azo-M13 phage (in water) upon exposure to UV light of 365 nm (5 min intervals; C = 0.002 g/mL in H_2O; 27°C) at different times (0–20 min). Due to photo-induced isomerization upon exposure to UV light, there is a gradual decrease in the absorbance at ~312 nm (in trans form) and a corresponding gradual increase in the absorbance at ~230–240 nm (π–π*, cis form), suggesting the trans-to-cis configurational change of the azo on the phage during light exposure. Appearance of isopestic points (i.e., points of equal absorbance) indicates that photochemical changes are solely due to isomerization. The spectrum of the methoxy-azo-M13 phage in cis form is recovered to that in its initial trans configuration (Fig. 3) after a few hours of UV irradiation and then in dark.

aromatic substitution for the formation of azo groups. Towards this end, we first fused a tyrosine-terminated decapeptide (amino acid sequence: Y-Y-G-Y-Y-G-Y-Y-G-Y) (Supporting information, Fig. S1) to the N-terminus of pVIII of M13 phage to facilitate the diazotization coupling reaction[23,24] of the tyrosine ring with the aromatic amines (Fig. 1c). When aromatic amine is allowed to interact with a high density of tyrosine (Y) residues under optimal conditions, we observed the formation of an azo chromophore (Figs. 2 and S2). The mechanism involved in the formation of azo chromophore is a diazotization coupling reaction[25].

The diazotization reaction offers an easy way to develop photo-responsive azo-M13 phage bioconjugate. We covalently conjugated 2 different aromatic amines (with methoxy, $-OCH_3$, or nitro end, $-NO_2$) with the tyrosine end of the peptides displayed on the phage to form two types of complex, which are termed methoxy-azo-M13 or nitro-azo-M13 depending on the aromatic amines used. Structural and photo-responsive properties of the resultant azo-M13 phage were investigated. The reaction scheme and detailed experimental procedures are shown in supporting information (Fig. S2a). The diazotization reaction results in the formation of a new –N=N– link between

the p-substituted aromatic amine and ortho position of the tyrosine ring, leading to the introduction of azo units to the phage structure.

Photoresponsive behavior of azo M13 phage. Azo polymers are famous for their light or thermal induced trans-cis isomeric characters, as compared with other chromophores. They have two types of isomeric forms, trans and cis, which show different steric structures, absorption spectra and dipole moments. The amount of trans and cis isomers of the azobenzene molecules can be controlled by applying light at a certain wavelength or heat. Until now three types of mechanism have been proposed for trans-to-cis isomerisation of azobenzene molecules such as rotation, inversion, and concerted-inversion of the N=N or N=N-C bonds[26,27]. In the present work we observed that the azo-M13 phage shows a reversible photo-responsive behaviour (Figs. 2 and 3), which is due to the photo-switchable cis-trans isomerisation of the azo chromophores introduced after bioconjugation[28,29]. The incubation of an aqueous solution (0.002 g/mL) of the azo-M13 phage in dark served to maximize the absorption at ~390 nm (nitro-azo-M13 phage; Fig. S3) or at 312 nm (for methoxy-azo-M13 phage; Fig. 3), which is corresponding to the trans azo chromophore. The irradiation of the solution of methoxy or nitro-ended azo-M13 phage was performed with 365 nm UV light, which was obtained from a UV lamp coupled with a monochromator. Upon UV light irradiation, the energetically preferred ground state (*trans*-form) goes to the cis-form via a photochemical trans-to-cis isomerisation process (Fig. 2), as evidenced by a gradual decrease in the absorbance at ~312 nm (for methoxy-azo-M13 phage; Fig. 2) or ~390 nm (for nitro-azo-M13 phage; Fig. S3), which is due to π–π* transition of the trans isomer and the corresponding increase of the absorbance at ~230–250 nm (due to π–π* transition of the cis isomer) with time. This change in absorption spectra confirms the transformation of the azo chromophore from trans to cis isomer on the azo-M13 phage upon UV light irradiation. In order to demonstrate the cis to trans transformation (i.e., reversible process) of the azo chromophore on the azo-M13 phage, after 20 min UV irradiation of the methoxy-azo-M13 phage, the sample was maintained in the dark at room temperature and the absorption spectra were measured. It is observed that, at room temperature, the spectrum of the methoxy-azo-M13 phage started to regenerate to its initial trans configuration (Fig. 3; dotted line spectra was taken after 4 h). This cis-to-trans isomerisation process (due to thermal relaxation) is much slower than the trans-to-cis photoisomerisation process. The observed slow cis-trans relaxation of the azo units in the highly rigid azo-M13 phage surface can be attributed to the conformational changes associated with the isomerisation in a constrained geometry. This behaviour is usually observed in the photoisomerisation of the conventional azo polymer systems[30,31]. It is worth noting that the observed cis-trans slow relaxation due to the conformational changes associated with the isomerisation in a constrained geometry, was previously documented in literature for conventional azo polymers[30,31]. We hypothesize that the conjugated molecules on the phage are smaller than the diameter of the phage. Thus, their conjugation and isomerisation will not induce the morphological change of the individual phage nanowires when they are non-aggregated[32].

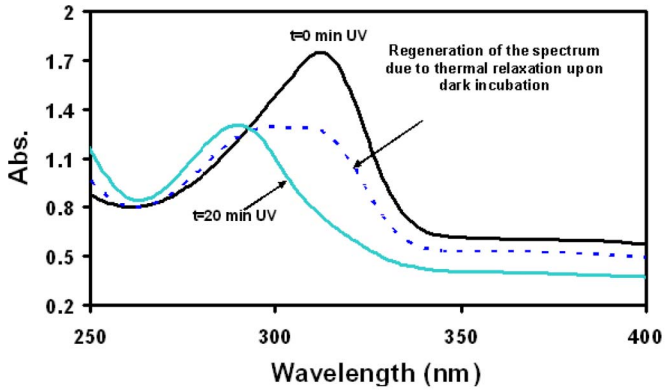

Figure 3 | Reversible change in the absorption during the cis-trans isomerisation on the methoxy-azo-M13 phage. Top black curve: absorption spectrum of the methoxy-azo-M13 phage (with azo in trans configuration) before it was irradiated by UV light. Bottom blue curve: Absorption spectrum of the methoxy-azo-M13 phage after 20 min UV irradiation. Middle dashed line: absorption spectrum of the methoxy-azo-M13 phage that was first irradiated for 20 min and then kept in the dark at room temperature, which shows that the spectrum of the UV-exposed methoxy-azo-M13 phage with azo in cis configuration starts to recover to that with azo in its initial trans configuration after a few hours due to thermal relaxation and was found to be slower than the trans-cis photoisomerisation. Observed slow cis-trans relaxation can be attributed to the conformational changes associated with the isomerisation in a constrained geometry, which is previously documented in literature for conventional azo polymers. The reversible cis-trans configurational transformation (Figs. 2 and 3), called trans-cis isomerisation, is well known in the case of conventional polymers, but has never been established on the virus system.

The morphology of phages before and after chemical modification was examined by transmission electron microscopy (TEM) analysis. The TEM images of phage before and after modification with methoxy ended azo groups were shown in Fig. 4. It was found that the morphologies of individual phage nanowires were almost not changed due to the peptide display or chemical modification, further verifying the chemical stability of phage. However, the color of the suspension of phage nanowires was changed from colorless to yellow due to the formation of azo dye after modification (Fig. 4, inset), which is consistent with the UV-Visible absorption spectral change after chemical modification (Fig. S2b). Similar color change was observed when aromatic amine with R=$-NO_2$ was used for the conjugation with tyrosine displayed on the side walls of phage nanowires.

Structural characterization of engineered M13 phage and azo-M13 phage. The FTIR spectra of engineered M13 phage (Fig. S4a) and azo-M13 phage (Fig. S4b) in purified and freeze-dried forms were measured. The characteristic peak due to the azo linkage (−N=N−) attached to tyrosine ring is identified at ~1508 cm^{-1} [33,34] and methoxy peaks are identified at 1246 and 1036 cm^{-1} in the methoxy-azo-M13 phage. In the case of nitro-azo-M13 phage, the azo linkage (−N=N−) identified between 1519–1479 cm^{-1} is found to be coupled with NO_2 stretching. The nitro end in the nitro-azo-M13 phage can be found at ~1519.15 cm^{-1} and 1343 cm^{-1} (Fig. S4b). The appearance of the peak at 860 cm^{-1} is attributed to –C-N stretching[35] and the peaks at 753.9 and 692.7 cm^{-1} are due to the

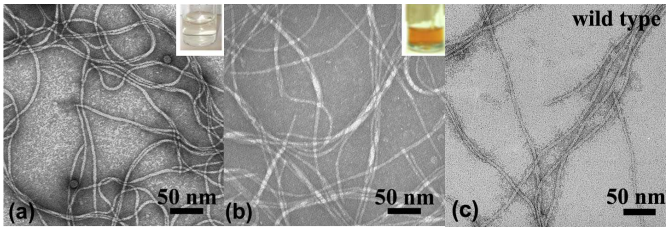

Figure 4 | TEM images of phage nanowires before (a) and after (b) conjugation with aromatic amine to form methoxy- ended azo groups on the side walls. The insets in (a) and (b) show the sample bottles of the corresponding suspensions of the phage nanowires, indicating the color change due to the formation of azo dye units on phage. (c) TEM image of wild type M13 phage.

out-of-plane C-H bending of 1,4-disubstituted benzene rings and ortho substituted rings[36]. These results further verify the successful coupling of aromatic rings onto the surface of the engineered M13 phage, resulting in the formation of azo chromophore (Fig. 1c).

Further, proton NMR study of the engineered M13 phage and methoxy-azo-M13 phage was carried out in D_2O to confirm the structural changes observed above. The NMR spectra for the engineered M13 phage and methoxy-azo-M13 phage were collected in 90% D_2O with the residual HDO peak referenced to 4.78 ppm (Figs. 5 and S5). The peaks at 6.92 and 7.22 ppm are corresponding to the tyrosine residues displayed on the engineered M13 phage (Fig. S5 a–b). Two aromatic rings (Ring A and B) will be expected in the azo-phage due to the conjugation between aromatic amine and tyrosine-displayed phage (Fig. 1c). The protons on Ring A (indicated in Fig. 1) were determined to be 7.33 and 7.65 ppm (Fig. S5 c–d). The peaks arising from the methoxy-azo-M13 phage (Fig. S5 c–d) were observed at 3.84, 6.93, 7.0, 7.27, 7.33, and 7.6 ppm. The partial gCOSY 2D NMR spectra of the engineered M13 phage and methoxy-azo-M13 phage were measured to further confirm the conjugation of the aromatic amines with the tyrosine to form azo chromophore on phage (Fig. 5a–b). The off-diagonal peaks between the tyrosine resonances (Fig. 5a) represent the coupling between the protons on the tyrosine ring on the engineered M13 phage. The off-diagonal peaks between 7.33 and 7.65 ppm in the COSY spectra represent the large ortho coupling between the protons in methoxy-azo-M13 phage (Fig. 5b). The chemical shifts of the protons of ring B (indicated in Fig. 1) are found to be at 6.93, 7.0 and 7.27 ppm. The large off-diagonal peak between 6.93 and 7.0 ppm represents the large ortho 3 bond coupling of the proton, while the smaller off-diagonal peak between 7.0 and 7.27 ppm corresponds to the smaller meta coupling of the ring protons. Integration of the area of the peaks gives 3 protons for 3.84 ppm, 2 protons for 7.33 and 7.65 ppm, and 1 proton for 6.93, 7.0 and 7.33 ppm. These integrated values were consistent with the resonance assignments. These results confirm the conjugation of amines with phage (Fig. 1c). The full proton spectra are shown in Figs. S5a and c for engineered M13 phage and methoxy-azo-M13 phage, respectively.

Discussion

The above results show that we have adopted a unique strategy for making photo-responsive phage, which is entirely different from other reports on making photo-responsive biomolecules[18–21]. In the most of the approaches reported so far, the azo dye is first synthesized with active end groups and further attached to biomolecules or polymer surface. In current approach, we simply used phage display technique to install a huge number of aromatic tyrosine rings on the surface of phage via molecular cloning and the conjugation of aromatic amines with the tyrosine rings forms an azo bond (Fig. 1), making phage photo-responsive (Fig. 2). Therefore, our new approach integrates modern molecular biology, phage biotechnology and classic organic chemistry to convert phage into a functional organic nanomaterial. The display of the decapeptide with an amino acid sequence Y-Y-G-Y-Y-G-Y-Y-G-Y on the N-terminus of major coat proteins of phage was confirmed by DNA sequencing result (Fig. S1). The UV-Vis (Fig. S2b), FT-IR (Fig. S4) and NMR (Figs. 5, and S5) spectra collectively indicate the formation of azo bond via diazo coupling reaction as shown in Fig. 1.

This work represents the first report on the conversion of the filamentous phage into a photoresponsive organic material. Use of phage for photo-responsive organic dye applications is superior to other synthetic or natural polymers for the following reasons: (1) Phage is nontoxic to human beings and recent studies show that filamentous phage is a new workhorse in biomedicine and has been placed into animal and human bodies for disease treatment[5,37–41];

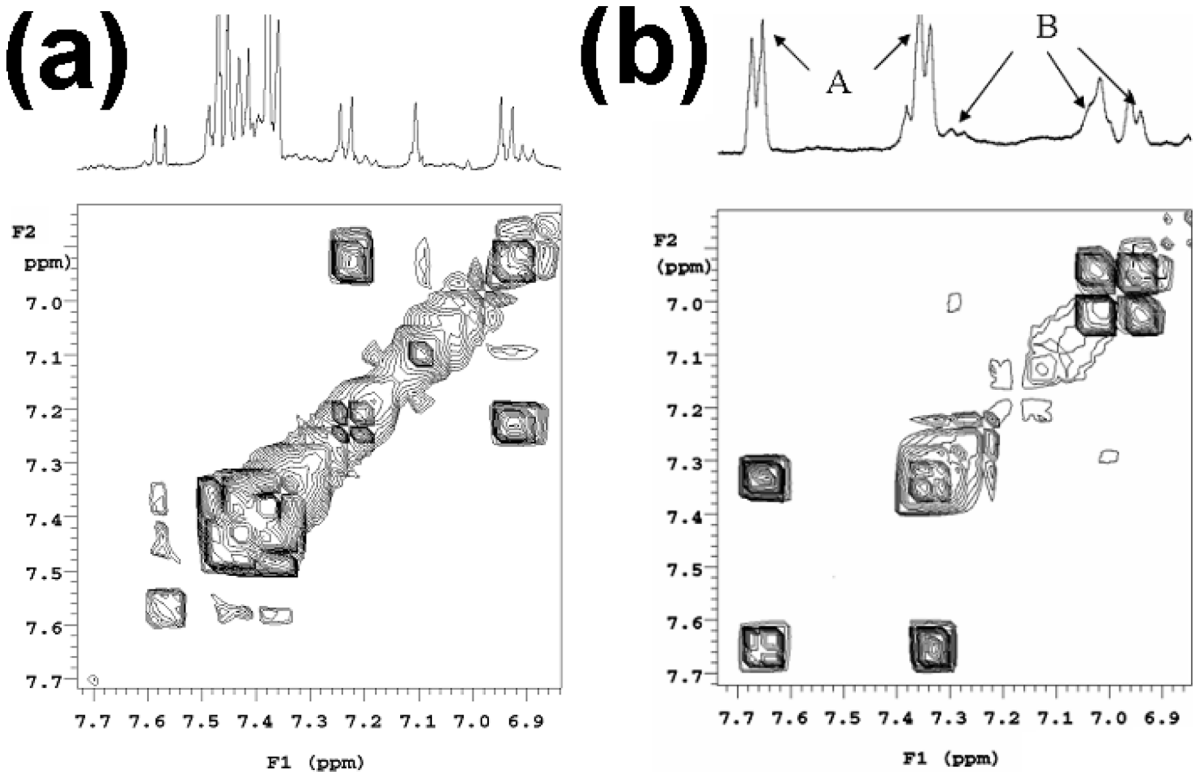

Figure 5 | Partial gCOSY NMR spectra of the engineered M13 phage (left) and methoxy-azo-M13 phage (right). The off-diagonal peaks between 7.33 and 7.65 ppm in the COSY spectra represent the large ortho coupling between the protons (a) and large off-diagonal peaks between 6.93 and 7.0 ppm represent the large ortho 3 bond coupling of the proton from the additional aromatic ring (b), while the smaller off-diagonal peak between 7.0 and 7.27 ppm corresponds to the smaller meta coupling of the ring protons of ortho substituted tyrosine ring. This observation indicates azo chromophore formation on the ortho position of tyrosine ring of the engineered M13 phage.

(2) It is chemically stable in various media (most acid, basic, and organic solvents) and thermally stable up to 80°C[32]; (3) By infecting bacteria, it can be amplified in bulk cost-efficiently, leading to a yield of phage up to 300 mg per liter of cell culture. Namely, bacteria are natural factories for the error-free mass production of monodisperse phage particles. Thus, phage is extremely monodisperse as compared to conventional polymer systems[4,32]; (4) The surface density of phage (as high as 300–400 m^2/g) is higher than the currently used catalysts[32]; (5) It has been demonstrated that M13 phage can self-assemble into a lyotropic liquid crystal, which can be further converted into a free-standing liquid crystalline film[4,6,7,42,43], due to the filamentous shape and monodispersity.

The reversible photo-isomerisation associated with photo-induced birefringence and dichroism, usually found in conventional azo-based photo-chromic materials, is the foundation of using azo polymers in technical applications such as non-linear optics (NLO)[44], photomechanical systems[45], photo switches, holographic data storage devices and micro patterning[17,46]. The robust photo-induced trans-cis isomerization of the azo polymers can cause significant bulk and surface property variation of the polymers, such as photoinduced phase transition, photoinduced anisotropy, and photoinduced surface relief gratings (SRGs)[47]. Holography is a three dimensional information storage technique that can store both phase and amplitude of the light waves diffracted by an object. It is very promising as it offers volume-based data storage compared to conventional magnetic recording materials. The ideal recording medium should be cost-effective, eco-friendly, sensitive, reversibly recordable, with very high diffraction efficiency and without the need of post-treatment after recording[48] to advance the holography technique[49]. In this field, azo-based biopolymers are attractive candidates for building holography data storage media[21]. Because M13 phage can self-assemble into ordered 2D or 3D materials[6], we expect that our new photo-responsive azo-M13 phage conjugates and the higher-order materials assembled from them will show promising reversible photoresponsive properties, enabling their application in non-linear optics, optical data storage and reversible holography recording.

In conclusion, we have demonstrated that the filamentous phage can be converted into a novel photo-responsive dye-like nanowire. The novel optical properties result from the introduction of an azo chromophore to the body of phage due to the successful covalent conjugation of aromatic amines onto the tyrosine residues genetically displayed on the side wall of the phage. This bio-conjugation strategy indicates that site-directed phage mutagenesis (i.e., site-directed display of a specific foreign peptide) can lead to the site-directed chemical modification. With the capability of displaying a peptide terminated with any of the 20 natural amino acids and the rich bioconjugation chemical reactions available in the literature, our strategy represents a versatile approach to introducing an organic molecule to the phage body. In this strategy, either the conjugated organic molecules or the new bonds due to the bioconjugation (which is the case in this work) can contribute to the novel properties of the bioconjugated phage.

Methods

Display of tyrosine-bearing peptide on the major coat of phage. We followed our established protocol[15,50–52] to display a decapeptide with an amino acid sequence of Y-Y-G-Y-Y-G-Y-Y-G-Y on the major coat of M13 phage and amplify the engineered phage.

Conversion of M13 phage into a photo-responsive organic dye (Azo-M13 phage conjugate) by conjugation with aromatic amines. Two different azo-M13 phage conjugates with methoxy and nitro end group were prepared by a two-step reaction (Fig. S2a). The aromatic diazonium salt was prepared by diazotizing corresponding aromatic amine with sodium nitrite at 0°C and further coupling with the tyrosine units on the side wall of the engineered M13 phage at 0°C. Further reaction mixture was maintained at ~5°C for about 3 h with occasional vortexing and dialyzed against an aqueous phosphate buffer for 36 h using a 50 kDa molecular weight cutoff cellulose dialysis membrane. (See supporting information for detailed procedure).

UV/Visible spectroscopy and Photo-irradiation of azo-phage. Shimadzu-2401 PC spectrophotometer (USA) was used to record the UV-Visible absorption spectra of the samples. The irradiation of the azo-M13 phage was performed on the top of the spectrophotometer sample cavity with 4 watt compact UV Lamp (365 nm) (model number UVL-21, UVP, LLC, CA, USA) with a filter. The exposure time of the irradiation was changed from 0 to 20 or 40 min. The reversible photo-responsive nature of the azo-M13 phage was tested by measuring the UV-Visible spectrum of the azo-M13 phage maintained in the dark right after it was irradiated by the UV light.

Transmission electron microscopy (TEM) analysis. TEM images of unmodified and modified phage were captured with Zeiss (Germany) transmission electron microscopy with 80 kV accelerating voltage. The samples for this analysis were stained using uranyl acetate. Excess stain was removed by blotting, followed by rinsing again with double distilled water and drying in air.

FT-IR spectroscopic characterization of photo-responsive azo-phage. A Nicolet (Nexus 470) Fourier transform infrared (FT-IR) spectrophotometer was used to substantiate the formation of products in this study with dried potassium bromide pellets. The engineered M13 phage, methoxyl-azo-M13 and nitro-azo-M13 phage in purified and freeze-dried forms were measured.

^{1}H NMR study. All NMR spectra were collected on a Varian VNMRS 400 MHz NMR Spectrometer with VNMRJ 2.1B software. The proton spectra were collected with the PRESAT pulse sequence as supplied by Varian Inc. with a sweep width of 6410.3 Hz, acquisition time of 2.5 seconds, 2 second recycle delay and 3868 transients for the engineered M13 phage and 10200 transients for the methoxy-azo-M13 phage. The COSY spectra were collected with the gCOSY pulse sequence as supplied by Varian Inc. with 272 transients and 128 increments for both compounds. The spectra were collected in 90% D_2O with the residual HDO peak referenced to 4.78 ppm.

1. Cao, B. R., Xu, H. & Mao, C. B. Transmission electron microscopy as a tool to image bioinorganic nanohybrids: the case of phage-gold nanocomposites. *Microscopy Research and Technique* **74**, 627–635 (2011).
2. Wang, F. K., Cao, B. R. & Mao, C. B. Bacteriophage bundles with prealigned Ca2+ initiate the oriented nucleation and growth of hydroxylapatite. *Chemistry of Materials* **22**, 3630–3636 (2010).
3. Ngweniform, P., Abbineni, G., Cao, B. R. & Mao, C. B. Self-assembly of drug-loaded liposomes on genetically engineered target-recognizing M13 phage: a novel nanocarrier for targeted drug delivery. *Small* **5**, 1963–1969 (2009).
4. Dogic, Z. & Fraden, S. Ordered phases of filamentous viruses. *Current Opinion in Colloid & Interface Science* **11**, 47–55 (2006).
5. Pasqualini, R. & Ruoslahti, E. Organ targeting in vivo using phage display peptide libraries. *Nature* **380**, 364–366 (1996).
6. Lee, S. W., Mao, C. B., Flynn, C. E. & Belcher, A. M. Ordering of quantum dots using genetically engineered viruses. *Science* **296**, 892–895 (2002).
7. Mao, C. B. *et al.* Virus-based toolkit for the directed synthesis of magnetic and semiconducting nanowires. *Science* **303**, 213–217 (2004).
8. Nam, K. T. *et al.* Virus-enabled synthesis and assembly of nanowires for lithium ion battery electrodes. *Science* **312**, 885–888 (2006).
9. Lee, B. Y. *et al.* Virus-based piezoelectric energy generation. *Nature Nanotechnology* **7**, 351–356 (2012).
10. Li, K. *et al.* Chemical modification of M13 bacteriophage and its application in cancer cell imaging. *Bioconjugate Chemistry* **21**, 1369–1377 (2010).
11. Mao, C. B., Liu, A. H. & Cao, B. R. Virus-based chemical and biological sensing. *Angewandte Chemie International Edition* **48**, 6790–6810 (2009).
12. Wang, F. K., Nimmo, S. L., Cao, B. R. & Mao, C. B. Oxide formation on biological nanostructures via a structure-directing agent: towards an understanding of precise structural transcription. *Chemical Science* **3**, 2639–2645 (2012).
13. Zhu, H. B. *et al.* Controlled growth and differentiation of MSCs on grooved films assembled from monodisperse biological nanofibers with genetically tunable surface chemistries. *Biomaterials* **32**, 4744–4752 (2011).
14. Gandra, N. *et al.* Bacteriophage bionanowire as a carrier for both cancer-targeting peptides and photosensitizers and its use in selective cancer cell killing by photodynamic therapy. *Small* **9**, 215–221 (2013).
15. Xu, H., Cao, B. R., George, A. & Mao, C. B. Self-assembly and mineralization of genetically modifiable biological nanofibers driven by beta-structure formation. *Biomacromolecules* **12**, 2193–2199 (2011).
16. Browne, W. R. & Feringa, B. L. Making molecular machines work. *Nature Nanotechnology* **1**, 25–35 (2006).
17. Shibaev, V., Bobrovsky, A. & Boiko, N. Photoactive liquid crystalline polymer systems with light-controllable structure and optical properties. *Progress in Polymer Science* **28**, 729–836 (2003).
18. Shimoboji, T. *et al.* Photoresponsive polymer-enzyme switches. *Proceedings of the National Academy of Sciences* **99**, 16592–16596 (2002).
19. Vollmer, M. S., Clark, T. D., Steinem, C. & Ghadiri, M. R. Photoswitchable hydrogen-bonding in self-organized cylindrical peptide systems. *Angewandte Chemie International Edition* **38**, 1598–1601 (1999).
20. Cattani-Scholz, A., Renner, C., Oesterhelt, D. & Moroder, L. Photoresponsive dendritic azobenzene peptides. *ChemBioChem* **2**, 542–549 (2001).

21. Rasmussen, P. H., Ramanujam, P. S., Hvilsted, S. & Berg, R. H. A remarkably efficient azobenzene peptide for holographic information storage. *Journal of the American Chemical Society* **121**, 4738–4743 (1999).
22. Kehoe, J. W. & Kay, B. K. Filamentous phage display in the new millennium. *Chemical Reviews* **105**, 4056–4072 (2005).
23. Schlick, T. L., Ding, Z., Kovacs, E. W. & Francis, M. B. Dual surface modification of the tobacco mosaic virus. *Journal of the American Chemical Society* **127**, 3718–3723 (2005).
24. Romanini, D. W. & Francis, M. B. Attachment of peptide building blocks to proteins through tyrosine bioconjugation. *Bioconjugate Chemistry* **19**, 153–157 (2008).
25. Solomons, T. W. G. *Organic chemistry.* (John Wiley &Sons, 1988).
26. Bandara, H. M. D. *et al.* Proof for the concerted inversion mechanism in the trans→cis isomerization of azobenzene using hydrogen bonding to induce isomer locking. *Journal of Organic Chemistry* **75**, 4817–4827 (2010).
27. Diau, E. W. G. A new trans-to-cis photoisomerization mechanism of azobenzene on the S-1(n,pi*) surface. *Journal of Physical Chemistry A* **108**, 950–956 (2004).
28. Ghosh, S. & Banthia, A. K. Synthesis of photoresponsive polyamidoamine (PAMAM) dendritic architecture. *Tetrahedron Letters* **42**, 501–503 (2001).
29. Ghosh, S. & Banthia, A. K. Photoswitchable architectural polymer: toward Azo-based polyamidoamine side-chain dendritic polyester. *Journal of Polymer Science Part A: Polymer Chemistry* **39**, 4182–4188 (2001).
30. Liu, W. *et al.* Enzymatic synthesis of photoactive poly(4-phenylazophenol). *Chemistry of Materials* **12**, 1577–1584 (2000).
31. Buruian, E. C., Buruian, T., Airinei, A. & Robil, G. Photochromism of polyurethane cationomers with pendent azo groups. *Angewandte Makromolekulare Chemie* **206**, 87–96 (1993).
32. Petrenko, V. A. & Vodyanoy, V. J. Phage display for detection of biological threat agents. *Journal of Microbiological Methods* **53**, 253–262 (2003).
33. Hamciuc, E. *et al.* New poly(amide-imide)s containing cinnamoyl and azobenzene groups. *Polymers for Advanced Technologies* **17**, 641–646 (2006).
34. Kumaresan, S. & Kannan, P. Substituent effect on azobenzene-based liquid-crystalline organophosphorus polymers. *Journal of Polymer Science Part A: Polymer Chemistry* **41**, 3188–3196 (2003).
35. Li, M., Hu, Z., Chen, G. & Chen, X. Phase behavior of side-chain liquid-crystalline elastomers and their precursors containing para-nitro azobenzene. *Journal of Applied Polymer Science* **88**, 2275–2279 (2003).
36. Yang, S., Li, L., Cholli, A. L., Kumar, J. & Tripathy, S. K. Azobenzene-modified poly (L-glutamic acid) (AZOPLGA): Its conformational and photodynamic properties. *Biomacromolecules* **4**, 366–371 (2003).
37. Frenkel, D. & Solomon, B. Filamentous phage as vector-mediated antibody delivery to the brain. *Proceedings of the National Academy of Sciences* **99**, 5675–5679 (2002).
38. Carrera, M. R. A. *et al.* Treating cocaine addiction with viruses. *Proceedings of the National Academy of Sciences* **101**, 10416–10421 (2004).
39. Kolonin, M. G. *et al.* Synchronous selection of homing peptides for multiple tissues by in vivo phage display. *The FASEB Journal* **20**, 979–981 (2006).
40. Krag, D. N. *et al.* Selection of tumor-binding ligands in cancer patients with phage display libraries. *Cancer Research* **66**, 7724–7733 (2006).
41. Shukla, G. S. & Krag, D. N. Selection of tumor-targeting agents on freshly excised human breast tumors using a phage display library. *Oncology Reports* **13**, 757–764 (2005).
42. Zacher, A. N., Stock, C. A., Golden, J. W. & Smith, G. P. A new filamentous phage cloning vector: fd-tet. *Gene* **9**, 127–140 (1980).
43. Mao, C. B. *et al.* Viral assembly of oriented quantum dot nanowires. *Proceedings of the National Academy of Sciences* **100**, 6946–6951 (2003).
44. Yesodhaa, S. K., Pillai, C. K. S. & Tsutsumib, N. Stable polymeric materials for nonlinear optics: a review based on azobenzene systems. *Progress in Polymer Science* **29**, 45–74 (2004).
45. Camacho-Lopez, M., Finkelmann, H., Palffy-Muhoray, P. & Shelley, M. Fast liquid-crystal elastomer swims into the dark. *Nature Materials* **3**, 307–310 (2004).
46. Kawata, S. & Kawata, Y. Three-dimensional optical data storage using photochromic materials. *Chemical Reviews* **100**, 1777–1788 (2000).
47. Kim, D. Y., L, S. K. T., Li, L. & Kumar, J. Laser-induced holographic surface relief gratings on nonlinear optical polymer films. *Applied Physics Letters* **66**, 1166 (1995).
48. Schnabel, W. *Polymer and light.* (Wiley-VCH Verlag GmbH and Co. KGaA, 2007).
49. Coufal, H. J., Psaltis, D. & Sincerbox, G. T. *Holographic data storage.* (Springer, 2000).
50. Liu, A. H., Abbineni, G. & Mao, C. B. Nanocomposite films assembled from genetically engineered filamentous viruses and gold nanoparticles: nanoarchitecture- and humidity-tunable surface plasmon resonance spectra. *Advanced Materials* **21**, 1001–1005 (2009).
51. Mao, C. B., Wang, F. & Cao, B. Controlling nanostructures of mesoporous silica fibers by supramolecular assembly of genetically modifiable bacteriophages. *Angewandte Chemie International Edition* **51**, 6411–6415 (2012).
52. He, T., Abbineni, G., Cao, B. R. & Mao, C. B. Nanofibrous bio-inorganic hybrid structures formed through self-assembly and oriented mineralization of genetically engineered phage nanofibers. *Small* **6**, 2230–2235 (2010).

Acknowledgments

We would like to thank the financial support from National Science Foundation (CMMI-1234957, CBET-0854414, CBET-0854465, and DMR-0847758), National Institutes of Health (5R01DE01563309, 1R21EB015190-01A1, 4R03AR056848-03), Department of Defense Peer Reviewed Medical Research Program (W81XWH-12-1-0384), Oklahoma Center for the Advancement of Science and Technology (HR11-006) and Oklahoma Center for Adult Stem Cell Research (434003).

Author contributions

M.M. and C.B.M. conceived and worked out the concept, carried out the genetic and chemical modification of M13 phage, absorption, FTIR, NMR spectroscopy, and photo responsive characterization. G.A. involved in the genetic engineering of M13 phage and mass production of M13 phage. S.L.N. helped in the gCOSY NMR characterization and analysis of the results. B.C. conducted TEM characterization of phage. M.M., C.B.M., G.A. and S.L.N. discussed the results and wrote the manuscript.

Additional information

Supplementary information accompanies this paper at http://www.nature.com/scientificreports

Competing financial interests: The authors declare no competing financial interests.

How to cite this article: Murugesan, M., Abbineni, G., Nimmo, S.L., Cao, B. & Mao, C.B. Virus-based Photo-Responsive Nanowires Formed By Linking Site-Directed Mutagenesis and Chemical Reaction. *Sci. Rep.* **3**, 1820; DOI:10.1038/srep01820 (2013).